XLVI CILAMCE
VITÓRIA - ES - BRAZIL - 2025
XLVI IBERO-LATIN AMERICAN CONGRESS ON COMPUTATIONAL METHODS IN ENGINEERING

Numerical Modeling of Thin Plates under Perfectly Elastic-Plastic Behavior

Patrick Gomes Rodrigues[1], Flávio Augusto Xavier Carneiro Pinho[2]

[1]*Dept. of Something, Universidade Federal de Ouro Preto*
Ouro Preto, 35402-179, MG, Brasil
patrickgomesdm@gmail.com
[2]*Dept. of Something Else, Universidade Federal do Cariri*
Juazeiro do Norte, 63000-000, CE, Brasil
flavio.pinho@ufca.edu.br

Abstract. In engineering, the quest for a more efficient use of materials in design is increasingly common, often leading to analyses that extend beyond the linear elastic regime. Accordingly, this work presents an approach for two-dimensional area elements, where behavioral analysis begins with the creation of an algorithm that uses the Finite Element Method (FEM) for the discretization and calculation of variables of interest for the developed models. The study of material plasticity considers the von Mises yield criterion (1913), which is a function based on the second stress invariant for the occurrence of plastic deformations. Additionally, the material's physical behavior in this work accounts for the application of gradual loads to the element under analysis, transitioning the material from a fully elastic state to a perfectly plastic one. The reliability of the results is assessed by submitting identical models to a commercial software, Abaqus/Standard. As Abaqus also uses finite element analysis for its calculations, this comparison validates the accuracy of the results obtained from the developed algorithm.

Keywords: Elasticity, Plasticity, FEM.

1 Introduction

Project design for structural elements commonly simplifies the stresses imposed by assuming a linear elastic behavior of the constituent materials. However, most materials exhibit linear elastic behavior only up to a certain limit; once exceeded, the material operates in a different regime (e.g., plastic, viscous). Consequently, predicting this type of behavior is crucial for increasing the reliability and improving the use of materials in a project.

This work addresses the behavior of structural elements within an elastoplastic regime. Essentially, plasticity theory concerns solids that, after being subjected to a loading program, can sustain permanent (or plastic) deformations when fully unloaded (Souza Neto, Peric, & Owens, 2008).

According to Ding, Qin, and Cardew-Hall (2005), modeling with an elastoplastic regime can aid in a more complete use of material resources and provides an efficient method for calculating structural details related to their load-bearing capacity. Souza Neto, Peric, and Owens (2008) state that numerous engineering materials can be modeled using plasticity theory under conditions of practical interest, including metals, concrete, rocks, clays, and soils in general.

Building a constitutive model for the numerical analysis of structural elements fundamentally relies on laboratory tests. Only with experimental data can we accurately represent a material's physical behavior.

Throughout this work, the von Mises yield criterion (1913) is adopted for calculating the plastic components. This criterion establishes an analogy with elasticity, developing a plastic potential function from which the plastic strain increment is derived. Furthermore, the Finite Element Method (FEM), one of the most well-known and widespread analysis methods among structural analysis software, is used to analyze the behavior of the studied structural elements.

2 Linear Elasticity Theory

The concept of elasticity is summarized by two premises: the stress in the material is a unique function of the strain; and the material can fully recover to its "natural" shape after the applied forces are removed. Symbolically, the constitutive equation for elastic behavior in its most general form is written as:

$$\boldsymbol{\sigma} = \boldsymbol{G}(\varepsilon) \tag{1}$$

where $\boldsymbol{G}$ is a symmetric response tensor function and ϵ is a strain tensor. Considering that stress is a linear function of strain, that the strain gradient in the deformed material is small compared to unity (so the distinction between Lagrangian and Eulerian descriptions is negligible), and finally, assuming the infinitesimal strain tensor, the constitutive equation for linear elastic behavior can be written as

$$\sigma_{ij} = C_{ijkm}\varepsilon_{km} \;\; ou \;\; \boldsymbol{\sigma} = \boldsymbol{C\varepsilon} \tag{2}$$

known as the generalized Hooke's Law, where the elastic coefficient tensor C_{ijkm} has $3^4 = 81$ components. However, due to the symmetry of stress and strain tensors, it is evident

$$C_{ijkm} = C_{jikm} = C_{ijmk} \tag{3}$$

which reduces the number of distinct coefficients from 81 to, at most, 36.

When the elastic properties of a body, as described by the coefficients C_{ijkm}, are the same for all possible sets of reference axes at any given point, the material is said to be isotropic. For these materials, the constitutive equation has only two elastic constants.

Isotropy requires that the elastic tensor C in equation (2) be a fourth-order isotropic tensor. Generally, an isotropic tensor is one whose components do not change under any orthogonal transformation from one set of Cartesian axes to another. The most general fourth-order isotropic tensor can be expressed in terms of the Kronecker delta as

$$C_{ijkm} = \lambda\delta_{ij}\delta_{km} + \mu\left(\delta_{ik}\delta_{jm} + \delta_{im}\delta_{jk}\right) + \beta(\delta_{ik}\delta_{jm} - \delta_{im}\delta_{jk}) \tag{4}$$

where λ, μ, and β are scalars. However, since $C_{ijkm} = Cji_{km} = C_{ijmk}$, this implies that β must be zero for these symmetries. Therefore, substituting equation (4) into equation (2)

$$\sigma_{ij} = \left(\lambda\delta_{ij}\delta_{km} + \mu\delta_{ik}\delta_{jm} + \mu\delta_{im}\delta_{jk}\right)\varepsilon_{km} \tag{5}$$

which, by the substitution property of δ_{ij}, reduces the expression to

$$\sigma_{ij} = \lambda\delta_{ij}\varepsilon_{kk} + 2\mu\varepsilon_{ij} \tag{6}$$

which is Hooke's Law for isotropic elastic behavior. It is noted that for this behavior, the 21 constants of the generalized law are reduced to just two, λ and μ, which are known as the Lamé constants.

3 General Theory of Plasticity

A key assumption of small-strain plasticity theory is the decomposition of the total strain, ε, into the sum of an elastic component, ε e, and a plastic component, ε^e

$$\varepsilon = \varepsilon^e + \varepsilon^p \tag{7}$$

With the definition of an elastic domain delimited by a yield stress, a yield function, Φ, is introduced in the form

$$\Phi\left(\sigma, \sigma_y\right) = |\sigma| - \sigma_y \tag{8}$$

in which the elastic domain is defined as the set of stresses that satisfy $|\sigma| < \sigma_y$. It should be noted that at any stage a stress level above the current yield function is not allowed; that is, the plastically admissible stresses are located within the elastic domain or at its boundary. Any admissible stress must satisfy $\Phi(\sigma,\sigma_y) \leq 0$, so that for stress levels within the domain of the yield function, only elastic deformation can occur, while at its boundary, the

production of plastic deformation takes place.

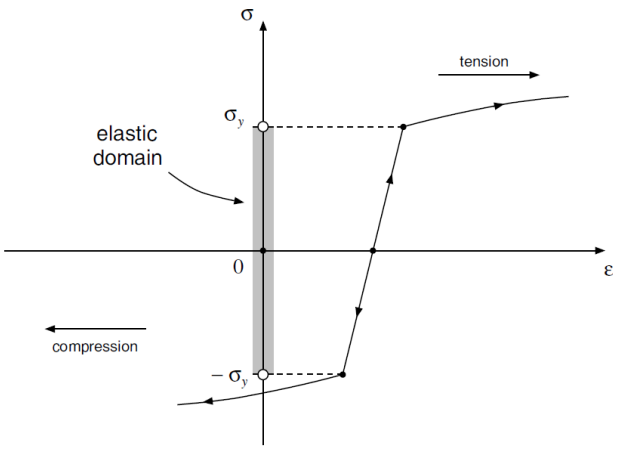


Figure 1 – Elastic domain of a uniaxial model (SOUZA NETO, PERIC, and OWENS, 2008).

In this analysis of plastic behavior, a perfectly plastic elastoplastic constitutive model was adopted, based on the von Mises yield criterion. This model disregards any type of hardening, assuming the material's yield stress remains constant after plastic deformation begins.

The associated plasticity flow rule, one of the Karush-Kuhn-Tucker (KKT) conditions, was used. This rule ensures that the direction of the plastic strain increment is orthogonal to the yield surface, which is consistent with the laws of thermodynamics.

For numerical integration, a return-mapping algorithm projected the stress state back onto the yield surface in a consistent manner. The consistent tangent stiffness matrix was then used in the Newton-Raphson scheme to ensure quadratic convergence of the iterative process and the accuracy of the solutions obtained.

3.1 Von Mises Yield Criterion

Proposed by von Mises (1913), the criterion states that the plastic regime begins when the second stress invariant, II_σ, reaches a critical value. This condition can be mathematically represented by the equation $II_\sigma = R(\alpha)$, where R is the critical value, here assumed to be a function of an internal hardening variable, α.

The uniaxial and shear stresses for von Mises theory are related in the following form

$$\sigma_y = \sqrt{3}\,\tau_y \tag{9}$$

where $\tau_y \equiv \sqrt{R}$ is the yield stress for shear.

The yield surface ($\Phi(\sigma)=0$) associated with the von Mises criterion is represented, in the principal stress space, by the surface of an infinite circular cylinder whose axis coincides with the hydrostatic axis. In the literature, the von Mises criterion (1913) is commonly associated with the Tresca criterion (1868) due to the compatibility between the two theories. However, the yield surface proposed by Tresca features points with abrupt changes in curvature, whereas the one proposed by von Mises presents a smooth curve, which justifies why only the von Mises criterion is presented in this work.

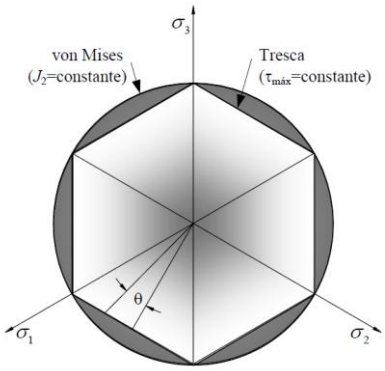


Figure 2 – Projections of the yield surfaces proposed by Tresca and von Mises (JORGE and DINIS, 2005).

4 Methodology

The "ARCO" algorithm, designed to numerically analyze the non-linear physical behavior of materials with an emphasis on perfect plasticity, was built using MATLAB®. This algorithm is based on the plane stress state and finite element discretization.

The implemented algorithm utilizes the von Mises yield criterion, making it suitable for the analysis of ductile materials. For verification purposes, comparative analyses are performed using the commercial software Abaqus/Standard, which also employs the Finite Element Method (FEM) in its calculation model. This comparison allows for an accuracy assessment of the developed code. The stages and methodology of this work are illustrated in Figure 3.

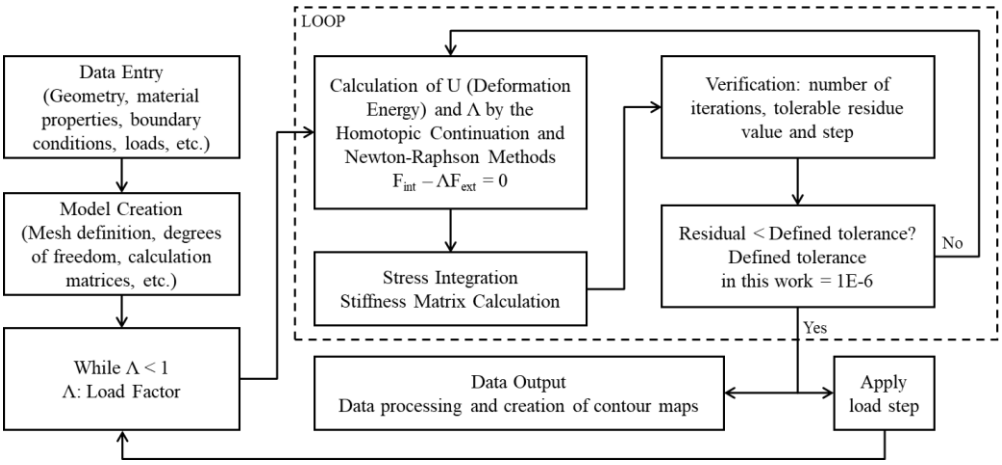


Figure 3 – Flowchart of the developed computational code.

One of the key result comparisons in this work involves contour maps generated by both ARCO and Abaqus/Standard. To ensure a direct comparison, the scales were made identical for both, matching both the color intensities and the value limits.

The model submitted to ARCO has a generic geometry. The material's stress-strain behavior is considered perfectly elastic-plastic, as shown by the curve in Figure 4. This curve illustrates a linear elastic regime up to a stress value equivalent to the material's yield stress, σ_y. Beyond this point, the material experiences strain (ϵ) without any increase in stress, forming a plateau in the curve

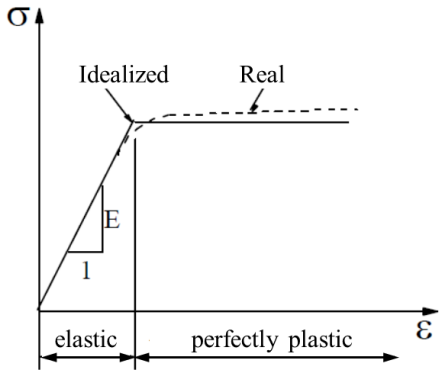


Figure 4 – Idealization of the perfectly elastic-plastic Stress-Strain relationship (MACHADO, 2005)

In this work, we chose a model with a generic geometry, defined as a thin plate element. These are elements of small thickness subjected to forces in their principal plane. The model is an L-shaped plate with a load q applied to one of its edges, parallel to the plate's principal plane.

The load q is applied incrementally until a limit load value supported by the piece is reached. This value is determined through both the developed code and the comparative software used.

The material properties are as follows:

- Elastic Modulus (E): 210 GPa
- Poisson's Ratio (ν): 0.3
- Yield Stress (σ_y): 250 MPa
- Thickness: 10 mm
- Maximum load (when fully imposed): 595 kN/m

Figure 5 schematically illustrates the model. It is important to note that the applied loads were determined using Abaqus/Standard, corresponding to a load intensity that produced a considerably noticeable level of plasticization in the element.

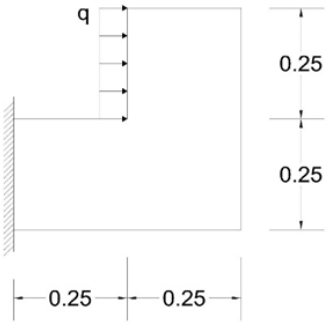


Figure 5 – Model scheme (units in meters)

5 Results

Figure 6 indicates the specific point and cross-section used as a basis for the numerical analysis within the model. These points were selected to obtain significant values for the variables of interest.

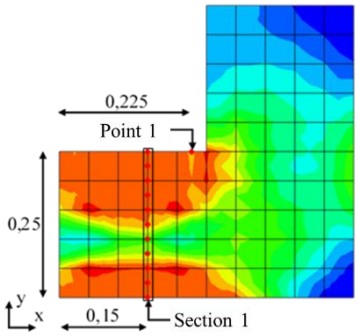


Figure 6 – Location of the chosen nodal points in the Model for data analysis

The displacements shown in Figure 7 are referenced only to Point 1 from Figure 5, as both directions exhibit significant displacement values at this same point. As observed in previous models, the variation in results for this model is also negligible, as shown in the following curve.

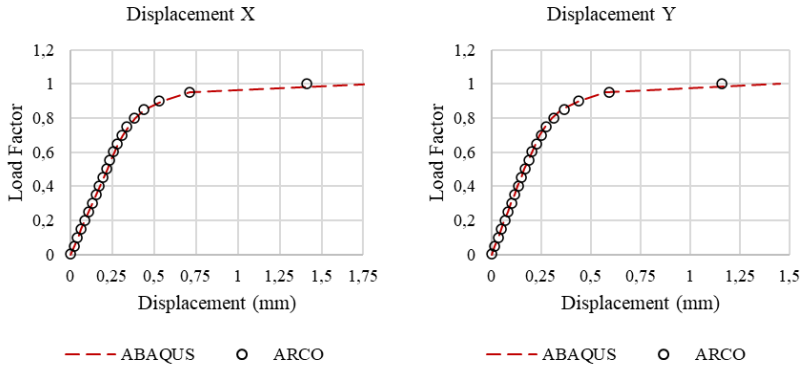


Figure 7 – Load-Displacement curves in the X and Y directions

The same holds true for the data presented in Figure 8, which illustrates the Stress-Strain curves. These curves can be used to quickly and easily determine the point at which the component transitions from the elastic to the plastic regime. The data from both models result in curves that are practically superimposed, with only insignificant variations, which further confirms the reliability of the results between the analyses.

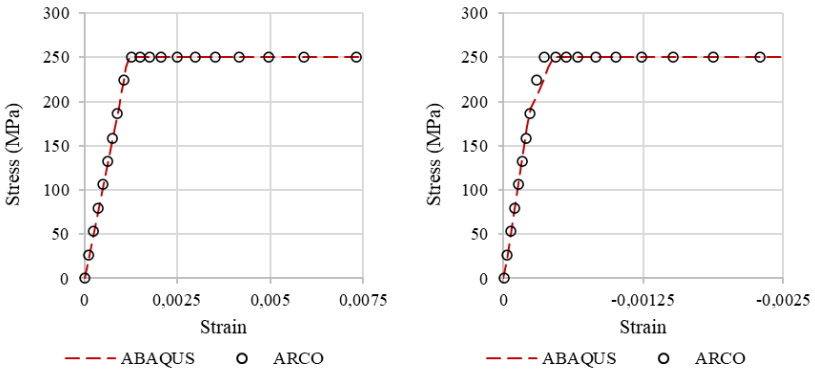


Figure 8 – Horizontal (left) and vertical (right) Stress-Strain curves at Point 1

This model accurately represents how the combination of principal stresses behaves within the yield surface after reaching the plastic regime, as can be seen in Figure 9. Here, the ordered pair of principal stresses, upon reaching the boundary of the domain imposed by the yield surface, begins to "travel" along it without exceeding it at all.

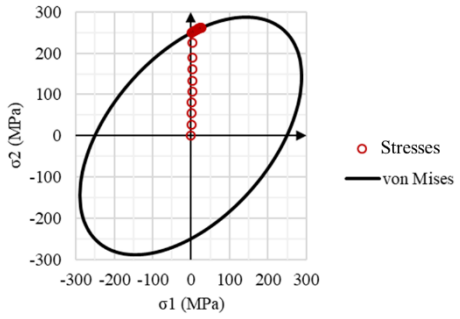


Figure 9 – Evolution of Principal Stresses (σ1 and σ2) at Point 1 within the yield surface.

The component's behavior and the regions with the highest stress levels can be identified in Figure 10. The regions marked in red on the color scale are those that have yielded or undergone plasticization. The figure also confirms the fidelity of the results from the ARCO algorithm when compared to Abaqus/Standard.

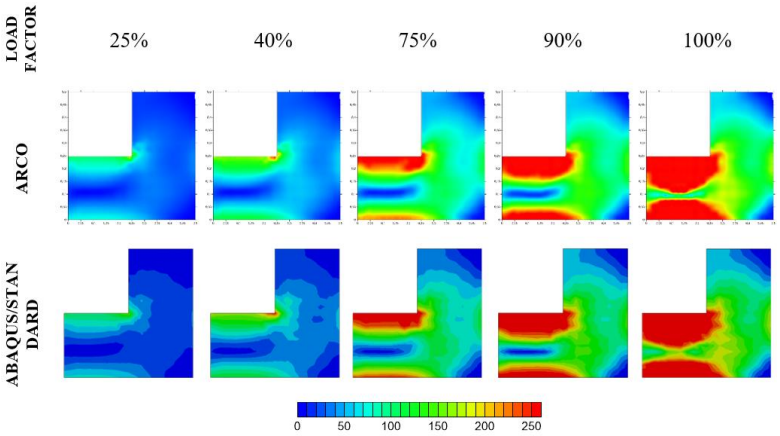


Figure 10 – Contour maps showing the evolution of von Mises stress in MPa

To provide a clearer understanding of how the component transitions out of its linear elastic regime during incremental loading, Figure 11 shows the axial stress diagrams for different load steps. Based on Section 1 from Figure 6, it is also possible to observe that the curves are nearly superimposed, with insignificant variations.

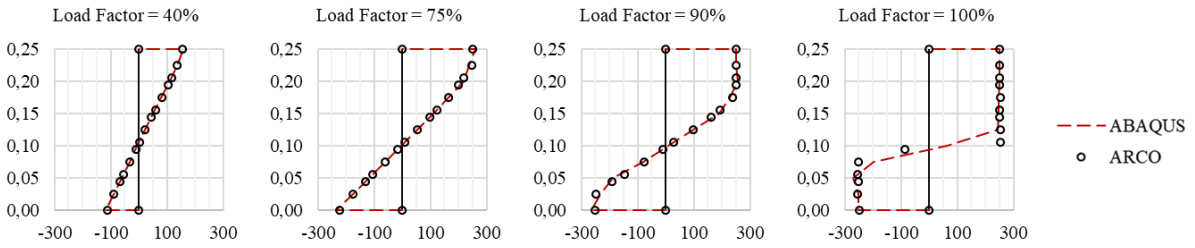


Figure 11 – Evolution of axial stresses in Section 1 of the Model's component (MPa)

6 Conclusion

Based on the presented analyses, it can be stated that the developed code demonstrates high reliability, as it provided satisfactory results when compared to those from the Abaqus/Standard software. This makes it a viable tool for designing components that make up structural elements in engineering.

It is important to highlight that this work focuses on a 2D plane analysis, whereas much of the structural analysis software deals with bar elements. This distinction underscores the complexity of implementing the proposed problem, particularly when coupled with the accuracy of ARCO's results compared to Abaqus/Standard, a widely used software in both academia and industry. This precision enhances the reliability of the proposed algorithm.

Therefore, ARCO proves to be a reliable tool for the structural analysis of two-dimensional elements, with potential applications in both project design and academic settings. It could serve as the foundation for developing a more elaborate software for structural engineering, representing the main contribution of this work.

Furthermore, this type of analysis contributes to greater economy and safety during the design of structural elements. Such a study can identify regions that need to be structurally reinforced or areas that contribute little to the resistance of applied loads. This is particularly valuable because plastic deformations are generally undesirable in structural components due to the loss of recovery capacity, a parameter that requires careful analysis.

It is important to emphasize that the complexity of the model can slightly hinder the analysis, as submitting a model requires familiarity with the MATLAB® programming language. Additionally, the hardware used can be a limiting factor for the algorithm's execution, given that the computational cost was not a parameter analyzed in this work, and the cost increases with model complexity.

A particular limitation of ARCO is its assumption of a non-hardening behavior. According to Baptista (2005), this simplification "can introduce considerable deviations in the referred stress-strain relationships, especially when the latter take on high values."

References

[1] ABAQUS, “User"s Manual”, Version 6.14-4, Dessault Systèmes Simulia Corp, Providence, RI, USA, 2014.
[2] ALLGOWER, Eugene L.; GEORG, Kurt. Introduction to Numerical Continuation Methods. Colorado State University: 1990.
[3] BAPTISTA, António M. Influência do endurecimento do material no cálculo das deformações de uma secção rectangular metálica em regime elastoplástico. In: V Congresso de Construçao Metálica e Mista. Portugal (Lisbon): CMM. 2005. p. 307-16.
[4] BAPTISTA, António Manuel. Formulação analítica do cálculo de secções de elementos estruturais metálicos em regime elastoplástico. In: VII Congresso de Mecânica Aplicada e Computacional. 2003. p. 449-458.
[5] COOK, R.D.; MALKUS, D.S.; PLESHA, M.E.; WITT, R.J. (2002). Concepts and Applications of Finite Element Analysis. 4ed. John Wiley & Sons, Inc.
[6] GURTIN, M. E. (1981). An introduction to continuum mechanics. (Mathematics in science and engineering). Academic Press, INC. Ltd. London, England. 265 p.
[7] JORGE, R M N; DINIZ, L M J S. Teoria da Plasticidade. Universidade do Porto: Faculdade de Engenharia, 2005.
[8] KRABBNHOFT, Kristian. BASIC COMPUTATIONAL PLASTICITY. Technical University Of Denmark: Departament Of Civil Engineering, 2002.
[9] MALVERN, L. E. (1969). Introduction to the Mechanics of Continuous Medium, Prentice Hall, Englewood Cliffs.
[10] MARCAL, P. V. (1971). Finite element analysis with material non-linearities-theory and practise, Recent Advances in Matrix Methods of Structural Analysis & Design, ed. R. H. Gallagher et al., The University of Alabama Press, pp. 257-282.
[11] MASE, G. T.; MASE, G. E. CONTINUUM MECHANICS for ENGINEERS. 2. ed. New York: CRC Press LLC, 2000.
[12] ODEN, J. Tinsley. NONLINEAR CONTINUUM MECHANICS. 3. ed., 2008.
[13] PIMENTA, Paulo Mattos. Fundamentos da Mecânica dos Sólidos e das Estruturas. São Paulo: 2006.
[14] SOUZA NETO, Eduard; PERIC, Djordje; OWENS, David. COMPUTATIONAL METHODS FOR PLASTICITY: THEORY AND APPLICATIONS. 1. ed. Wiley, 2008.
[15] VON MISES, R. (1913). Mechanik der Festen Korper im Plastische-deformablen Zustand. Göttin. Nachr. Math. Phys. volume 1, pp. 582–592.